University of Thi-Qar Journal of Science (UTsci)
The 4th Scientific Conference of Science College/ University of Thi_Qar
Volume (7), No.2

Enhancement Efficiency of Active Layer P3HT:POT:DBSA/PCBM Photoactive Solar Cell Device

Abdullah A. Hussein
Department of Material Science
Polymer research centre, university of Basrah
Basrah, Iraq
aahaat28977@yahoo.com

***Abstract*- In this work we have investigated thin film blend produced from regioregular poly(3-hexylthiophene) (rr-P3HT), Poly(o-toluidine) doped with dodecylbenzene sulphonic (POT:DBSA) and [6,6]-phenyl-C61 butyric acid methylester (PCBM) materials by spin coating method for application as active layer in photoactive solar cell (PSCs). A thin film uniform rr-P3HT:PCBM and rr-P3HT:POT:DBSA:PCBM were successfully deposited on the poly (3,4 ethylenedioxythiophene): poly (styrenesulfonate) (PEDOT:PSS) buffer layer substrate. The absorption spectra of the films were studied by using UV–vis spectrophotometer and Raman spectroscopy. the morphology of films is evaluated by X-ray diffraction (XRD) and atomic force microscopy (AFM) patterns. We have seen that, the efficiency enhancement for the device with a rr-P3HT:POT:DBSA:PCBM film is more significant than for the device with rr-P3HT:PCBM.**

***Keywords*— PEDOT:PSS, P3HT, POT:DBSA, PCBM, Photoactive Solar Cell.**

I. INTRODUCTION

Photovoltaic solar cells have been receiving significant consideration due to their easy manufacturing processing, flexibility and low cost (Shaheen et al., 2001). A complete understanding of the organic device physics, in particular bulk heterojunction structure using the blend of conjugated polymer and fullerene as the active layer constructed an efficient photovoltaic (PV) device because of ultra-fast charge separation from conjugated polymer to fullerene (Spanggaard et al., 2004; Sung-Ho et al., 2007), a highly increased interfacial area between the two components (Padinger et al., 2003), and the formation of percolation path for charge transport. In this case, the control of morphology on a nano-scale for each donor (D) and acceptor (A) phase of the thin composite film is known to play a crucial role for achieving high performance in the polymer solar cells (Ma et al., 2005). Theoretically, the arrangement of bulk hetero-junction phase allows for bulk separation of photo-induced excitons and high-mobility removal of electron through the phase. P3HT has been used p-type material (Li et al., 2005; Sirringhaus et al., 1998) in polymer solar cells along with a fullerene derivative, PCBM as an electron acceptor. Since hole is typically the high-mobility carrier in P3HT (Prosa et al., 1992), the enhanced electron mobility was achieved by addition of electron acceptor. However, the intricacy in bulk hetero-junction systems arises when we account for the effects of morphological modifications in P3HT phase because the introduction of phase (Chirvase et al., 2004). There are significant many of papers that investigate the effects of processing parameters on composite and blended solar cells nanophase (Chirvase et al., 2004; Schilinsky et al., 2005). Even, degree of regionregularity and the molecular weight (Kim et al., 2006; Brabec et al., 2001) of P3HT also affect the performance of P3HT:PCBM solar cell devices. Generally, the electric power extracted from a solar cell device depends on both the photocurrent and photovoltage of the diode circuit under illumination of a given intensity. In order to increase the power conversion efficiency (PCE) of a solar cell device, the practicable approach is to increase the photocurrent as much as possible, since the solar cell is limited by the built-in potential and it is the difference between LUMO and HOMO of the electron acceptor and donor materials (Hou et al., 2006). Interface morphologies and Different device geometries are evaluated for the purposes of trapping increase the light, dissociating of excitons more efficiently, transporting charges and more photocurrent (Shrotriya et al., 2005).

II. EXPERIMENTAL DETAILS MATERIALS

Poly (3-hexathiophine-2,5-diyl) (P3HT) (5 mg/mL,), Poly (O-toluidine) doped with dodecyl benzene sulfonic acid (POT: DBSA) (5mg /mL), and [6,6]-Phenyl C61 butyric acid methyl ester (PCBM) (10 mg/mL) are prepared in a solvent of chloroform (CF) in 0.5:0.5:1wt%. Poly (3,4-ethylenedioxythiophene) polystyrene sulfonate (PEDOT:PSS) 1.3 wt% dispersion in H2O (conductive grade) used without purification. Devices were fabricated using ITO coated glass slides with 120 nm thick, and 15Ω/sq sheet resistance from the same supplier.

III. PREPERATION METHOD

ITO coated glass slides were cleaned using DI water, acetone and isopropyl alcohol for 10 min each in an ultrasonic bath, respectively, and then blown dry in N2 gas. ITO surface was modified by spin coating to form a thin layer of hole transport PEDOT:PSS, followed by dried on hotplate for 15 min at 100oC in ambient air. Afterwards, the

mixed solutions consisting of P3HT, POT: DBSA and PCBM was used as supplied chloroform (CF) solvent in 0.5:0.5:1weight ratio were spin cast in a nitrogen-filled glove-box, with thickness of the active layer are 140nm. The solutions were stirred overnight at 50oC followed by filtering the P3HT:POT:DBSA:PCBM solutions through a PTFE filter with pore size of 0.45µm. Finally, a bilayer cathode consisting of 100 nm Al was thermal evaporated under high vacuum of ~ 1×10-6 Pa with a rate of 0.25 nm/s onto the polymer layer as a cathode to create a device with an active area of (8mm2) defined by a shadow mask on the active layer to form cells with an active area of 1cm2.

IV. MEASURMENTS

UV-vis absorption spectra of the polymer films were recorded on (Cecil Aquarius CE-7200) double beam spectrophotometer in the range of 190–900 nm was used to study the absorption spectra of films. Raman spectra were measured using a Renishaw RM1000 NIR 780TF diode laser (λ=514 nm) with (Pmax =15mW), and Aluminum substrate was used for the Raman spectroscopy measurements. The blend structures were examined by multipurpose X'Pert PHLIPS X-Ray defractometer (MPD) (Cu, k = 0.154nm). The films' morphology films were acquired using a BRUKER NanoScope IVmultimode atomic force microscope (Bruker-AFM) with the tapping mode, an Infinite Focus Microscope (IFM) and a FEI-Nova SEM scanning electron microscope. All fabrication steps and characterization measurements were performed at an ambient atmosphere. Thickness of the thin films was measured using a spectroscopic ellipsometry (M2000V -J.A. Woollam Co., Inc.) is operating in the wavelength range 350-850 nm. The photovoltaic properties were studied using a computer-controlled Keithley 6517A digital source meter and the photocurrent was generated under AM 1.5G irradiation source of 100 mWcm-2. A bias voltage is swept typically between (-0.1V) to (+ 0.1V) with a step of 0.5 mV. The mounting table and the spring probe pins with magnetic bases were designed and constructed in the lab. The data given in this paper were verified by making each device more than three times. The Power Conversion Efficiency (PCE) of the solar cells were evaluated using the following equations [Chirvase D.et al..(2004)]:

$$PCE\ (\%) = Jmax \times Vmax / Pin \quad (1)$$

$$FF(\%) = (Jmax \times Vmax) / (Jsc \times Voc) \quad (2)$$

Where Jmax and Vmax are the current density and voltage at the maximum power point, Jsc the short circuit current density, Voc is the open circuit voltage, the Pin is the power of incident light, and FF is the fill factor.

V. RESULTS

The optical transmittance spectra of PEDOT:PSS films provided in figure (1) is taken from the sample 40nm within the wavelength range (300–800 nm). Generally, the spectra of PEDOT:PSS films clearly show high optical transmittance which is suitable for the preparation of organic solar cell. is very high (i.e absorption very low), as a result it is transparent to (AM 1.5) radiation. Transmittance is ~ 95% in the visible range for layer PEDOT:PSS thin film.

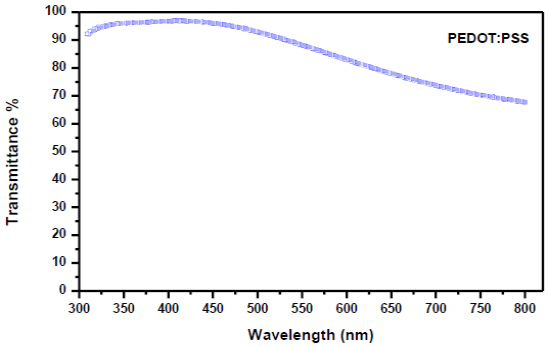

Fig. 1. Transmittance spectrum of PEDOT:PSS film

To investigate effects of the POT:DBSA on the PSCs, the photovoltaic characteristics of PSCs with and without POT:DBSA were measured and compared. Figure .(2) shows a schematic illustration of the fabricated PSCs consisting of a P3HT:PCBM and P3HT:POT:DBSA:PCBM active layer blend and the PEDOT:PSS with the PSS. We investigated the effect of POT:DBSA on the photovoltaic characteristics of the PSCs. Thin films of P3HT:PCBM and PEDOT:PSS/P3HT:POT:DBSA:PCBM, for UV–vis absorption within the wavelength range (300– 800 nm), studies were prepared glass substrate. It is clearly observed that, The active layers have exhibited typical absorption spectra that are divided into two main regions for both films; the first region around the wavelength ~395-650 nm was related to the absorption of the P3HT and POT:DBSA while the main absorption spectra below around the wavelength range of 290-390 nm was attributed to the PCBM molecules in the blend (Hoppe *et al.*, 2004). The spectral region associated with P3HT:POT:DBSA absorption showed three different bands, the main peak around at ~493 nm is attributed to the π–π* electronic transition in crystalline π-π stacking structure of P3HT:POT:DBSA chains main polymer conjugated polymer, and the absorption shoulder at ~ 545, 605 and 652 nm confirms the inter-chain absorption in the P3HT:POT:DBSA:PCBM material.(Schilinsky *et al.*, 2005).

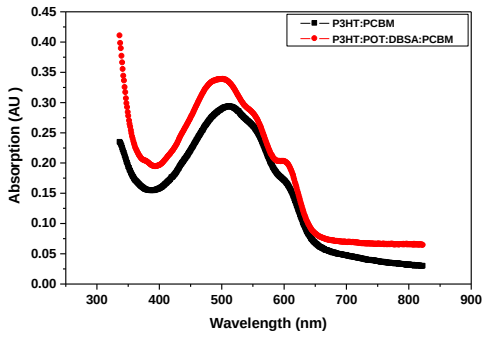

Fig. 2. UV–vis absorption spectra of P3HT:PCBM and films P3HT:POT:DBSA:PCBM.

Figure (3) shows the XRD pattern of P3HT:PCBM and P3HT:POT:DBSA:PCBM thin films, within the wavelength between 300 nm and 800 nm deposited on ITO glass substrate. The XRD intensity values were obtained peaks at $2\theta \approx 5.01^{o}$ for P3HT:PCBM and $2\theta \approx 5.12^{o}$ for P3HT:POT:DBSA: PCBM, where the reflection of (d_{100}-spacing) plane correspond to as describe by the (JCPDS 44-0558) (Kim *et al.*, 2006; Shrotriya *et al.*, 2005). These values

are corresponding to the inter-chain spacing in P3HT associated with the interdigitated alkyl chains and indicating the degree of crystallinity of P3HT (Jilian *et al.*, 2012). Figure (4) shows the Raman spectroscopy of P3HT:PCBM and P3HT:POT:DBSA:PCBM thin films. It was characterized by Raman spectroscopy in the range 200-2000 cm^{-1} deposited on Al substrate. The Raman spectroscopy of P3HT:PCBM films doesn't differ from P3HT:POT:DBSA:PCBM film due to no Raman features attributable to films and absence effect of POT:DBSA on the PEDOT:PSS/P3HT:PCBM films. Therefore, The main in-plane ring skeleton modes are similar behaviour in P3HT:PCBM films previous, as below: at 1452–1468 cm^{-1} (symmetric C=C stretching mode) and at 1381-1391cm^{-1} (C-C intra-ring stretching mode), the inter-ring C-C stretching mode at 1200-1210cm^{-1}, the C-H bending mode with the C-C inter-ring stretch mode at 1180- 1200 cm^{-1}, and the C-S-C deformation mode at 720-740 cm^{-1}.Similar results were also observed by pure P3HT with CB solvent only (Shrotriya *et al.*, 2005; Erb *et al.*, 2005).

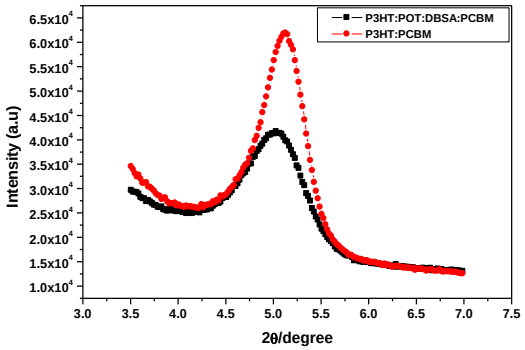

Fig. 3. XRD curves of P3HT:PCBM and P3HT:POT:DBSA:PCBM films

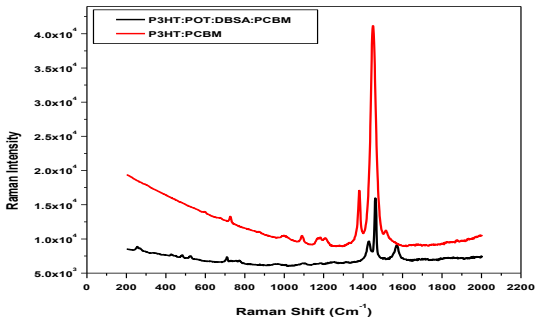

Fig. 4. Raman spectroscopy for P3HT:PCBM and P3HT:POT:DBSA:PCBM films

The active layer morphology of P3HT:PCBM and P3HT:POT:DBSA:PCBM thin films, deposited on a Si substrate, was investigated by atomic force microscopy (AFM). In order to understand the under laying morphology of the devices in the final photovoltaic cells, samples were made by removing the Al cathode from the final photovoltaic cells using sticky tape and the observed AFM images are displayed in figure (5). The root mean square roughness of the pristine P3HT:PCBM film is 6.7nm. The surface roughness increased to 8.2nm for the P3HT:POT:DBSA:PCBM thin film. The increased roughness and the observed different texture of the additive thin film POT:DBSA could be due to the presence of DBSA in the P3HT:POT:DBSA:PCBM layer which has undergone annealing process. The texture of the film P3HT:POT:DBSA:PCBM is similar throughout the surface of the film (Hugger et al., 2004).

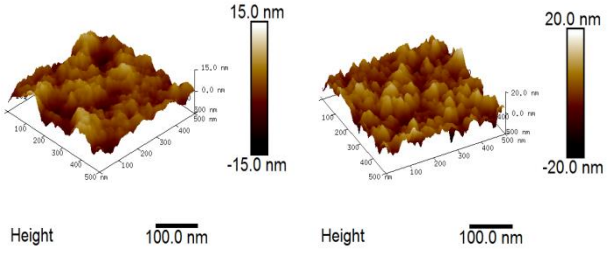

Fig. 5. AFM images of the P3HT:PCBM and P3HT:POT:DBSA:PCBM films.

TABLE 1 Summarizes the films' parameters as obtained from AFM image analysis; Ra is the film's mean roughness, Rmax the maximum height of the film and R.M.S is its root mean square

Sample	R. M. S(nm)	Ra (nm)	R_{max}(nm)
P3HT:PCBM	15.3	15.1	22.4
P3HT:POT:DBSA:PCBM	20.6	20.2	34.7

The current density versus voltage (J-V) characteristics of PEDO: PSS/P3HT: PCBM and PEDO:PSS/P3HT:POT:DBSA:PCBM devices were presented in Figure (6). Significant improvements show in the J-V characterization results of solar cells, especially on open-circuit voltage (Voc), current density (JSC) and fill factor (FF). The Voc was increased from 0.48 to 0.51 V, whereas the Jsc and FF were increased from 4.25 to 5.1mA/cm2 and 61% to 0.63%, respectively, for the PEDO:PSS/P3HT: POT:DBSA:PCBM photovoltaic cell device when compared to the PEDO:PSS/P3HT:PCBM photovoltaic cell device. The increase in PCE of PEDOT:PSS/P3HT:POT:DBSA:PCBM film can be attributed to presence of POT:DBSA throughout the active layer of P3HT:PCBM in film, which could increase the transport of charge carriers and increases in the interfacial contact area between the active layer and intermediate layer, which allowing more efficient hole collection at the anode, and hence increases Jsc and FF. This increases the PCE of the PEDO:PSS/P3HT:POT:DBSA:PCBM photovoltaic cell up to 2.06% compared to PEDO:PSS/P3HT:PCBM photovoltaic cell PCE of 2.55%.

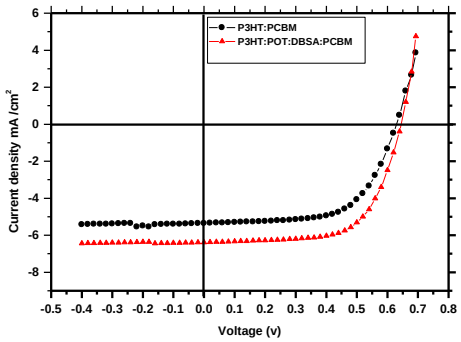

Fig. 6. (J–V) curves of PEDOT:PSS/P3HT:PCBM and PEDOT:PSS/ P3HT:POT:DBSA:PCBM films.

TABLE 2 Photovoltaic parameters for photovoltaic solar cell device.

Devices	Voc(v)	J sc(mA/ cm2)	FF (%)	PCE (%)
P3HT:PCBM	0.62	5.35	62	2.06
P3HT:POT:DBSA:PCBM	0.64	6.50	62	2.55

V. CONCLUSION

Organic solar cells with high efficiencies were fabricated using P3HT:PCBM and P3HT:POT:DBSA:PCBM. The inclusion of PEDOT:PSS buffer layer is thought to enhance light harvesting for the Organic solar cells of active layers. The effects of POT:DBSA on the performance of PSCs were investigated. The P3HT:POT:DBSA:PCBM has been shown to improve the morphology and crystallinity of the films, and therefore enhance the PCEs of the devices. the solar cells upon P3HT:POT:DBSA:PCBM give PCE of 2.06%, in contrast to 2.55% for devices.

IV. ACKNOWLEDGMENT

This research work was supported by Department of Material Science, Polymer Research Centre, University of Basrah

VII. REFRENCE

Brabec, C.J.; Cravino, A.; Meissner, D.; Sariciftci, N.S.; Fromherz, T.; Rispens, M.T. (2001). Origin of the Open Circuit Voltage of Plastic Solar Cells. Adv Funct Mater, 11:374.

Chirvase, D.; Parisi, J.; Hummelen, J.C. and Dyakonov, V. (2004). Influence of nanomorphology on the photovoltaic action of polymer–fullerene composites. Nanotechnology. 15:1317.

Coakley, K.M. and McGehee, M.D. (2004).Effect of device geometry on the performance of TiO2 nanotube array-organic semiconductor double heterojunction solar cells. Chem Mater, 16: 4533.

Erb, T.; Zhokhavets, U.; Gobsch, G.; Raleva, S.; Stühn, B. and Schilinsky, P. (2005). Correlation Between Structural and Optical Properties of Composite Polymer/Fullerene Films for Organic Solar Cells. Adv Funct Mater, 15: 1193.

Spanggaard, H. and Krebs, F.C. (2004). A Brief History of the Development of Organic and Polymeric Photovoltaics, Sol.Energy Mater. Sol. Cells 83: 125.

Hoppe, H.; Niggemann, M.; Winder, C.; Kraut, J.; Hiesgen, R.; Hinsch, A.; Meissner, D. and Sariciftci, N.S. (2004). Nanoscale Morphology of Conjugated Polymer/Fullerene-Based Bulk- Heterojunction Solar Cells. Adv. Funct Mater,14: 1005.

Hou, J.; Tan, Z.; He, Y.; Yang, C. and Li, Y. (2006). Synthesis and Photovoltaic Properties of Two-Dimensional Conjugated Polythiophenes with Bi(thienylenevinylene) Side Chains. Macromolecules, 39: 4657.

Hugger, S.; Thomann, R.; Heinzel, T. and Thurn-Albrecht, T. (2004). Semicrystalline morphology in thin films of poly(3-hexylthiophene). Colloid Polym Sci., 282:932.

Jilian, N.F.; Messai, A.M.; Manoko, M.; Willem, AL.O. and Neil, J.C. (2012). Ana Flavia Nogueira, Nanocomposites of gold and poly(3-hexylthiophene) containing fullerene moieties: Synthesis, characterization and application in solar cells.J. Power Sources, 215: 99-108.

Kim, J.Y.; Kim, SH.; Lee, H.H.; Lee, K.; Ma, W.; Gong, X. and Heeger, A.J. (2006). New Architecture for high‐efficiency polymer photovoltaic cells using solution‐based titanium oxide as an optical spacer. Adv Mater; 18: 572.

Kim, Y.; Cook, S.; Tuladhar, S.M.; Choulis, S.A.; Nelson ,J. and Durrant, J.R. (2006). A strong regioregularity effect in self organizing conjugated polymer films and high-efficiency polythiophene: fullerene solar cells. Nat Mater,5: 197.

Li, G.; Shrotriya ,V.; Huang, J.; Yao, Y. and Yang, Y. (2005). High- efficiency solution processable polymer photovoltaic cells by self-organization of polymer blends. Nat Mater, 4: 864.

Ma, W.; Yang, C.; Gong, X.; Lee, K. and Heeger, A.J. (2005). Thermally Stable, Efficient Polymer Solar Cells with Nanoscale Control of the Interpenetrating Network Morphology. Adv. Funct Mater, 15: 1617.

Padinger, F.; Rittberger, R. and Sariciftci, N.S. (2003). Effects of Postproduction Treatment on Plastic Solar Cells. Adv. Funct Mater, 13:85.

Prosa, T.J.; Winokur, M.J.; Moulton, J.; Smith, P. and Heeger, A.J. (1992). X-ray structural studies of poly(3-alkylthiophenes): an example of an inverse comb. Macromolecules, 25:4364.

Reyes-Reyes, M.; Kim, K.; Dewald, J.; Lopez-Sandoval, R.; Avadhanula, A.; Curran, S. and Carroll, D.L.(2005). Meso-structure formation for enhanced organic photovoltaic cells. Org. Lett., 7(26):5749-5752.

Schilinsky, P.; Asawapirom, U.; Scherf, U.; Biele, M. and Brabec, C.J. (2005). Influence of the Molecular Weight of Poly(3-hexylthiophene) on the Performance of Bulk Heterojunction Solar Cells. Chem. Mater, 17:2175-2180.

Shaheen, S.E.; Radspinner, R.; Peyghambarian, N. and Jabboura, G.E. (2001). Fabrication of bulk heterojunction plastic solar cells by screen printing. Appl. Phy. Lett., 79: 18.

Shrotriya, V.; Ouyang, J.; Ricky, J.T.; Gang, L. and Yang, Y. (2005). Absorption spectra modification in poly (3-hexylthiophene): methanofullerene blend thin films. Chemical Physics Letters, 411: 138–143.

Sirringhaus, H.; Tessler, N. and Friend, R.H. (1998). Integrated optoelectronic devices based on conjugated polymers Science, 280: 1741.

Sung-Ho, J.; Naidu, VK.; Han-Soo, J.; Sung-Min, P.; Jin-Soo, P.; Sung, CK. (2007). Optimization of process parameters for high- efficiency polymer photovoltaic devices based on P3HT:PCBM system, 91(13):1187–1193.

Van, J.; Yang, X.N.; Loos, J.; Bulle-Lieuwma, C.W.T.; Sieval, A.B.; Hummelen, J.C. and Janssen, R.A.J. (2004). Relating the Morphology of Poly(p-phenylenevinylene)/ Methanofullerene Blends to Solar-Cell Performance. Adv Funct Mater, 14: 425.

Yohannes, T.; Zhang, F.L.; Svensson, M.; Hummelen, J.C.; Andersson, M.R. and Ingana, O. (2004).Low-Temperature Combustion-Synthesized Nickel Oxide Thin Films, Thin Solid Films, 449:152.